JETIR.ORG ISSN: 2349-5162 | ESTD Year : 2014 | Monthly Issue
JOURNAL OF EMERGING TECHNOLOGIES AND INNOVATIVE RESEARCH (JETIR)
An International Scholarly Open Access, Peer-reviewed, Refereed Journal

Green Biosynthesis and Characterization of Cobalt and Iron oxide Nanoparticles Using Plant Extracts

Vipin Kumar* & Raman Kumar**
***Deptt of Physics, SKD University, Hanumangarh**
****Research Scholar, Deptt of Physics, SKD University, Hanumangarh**
Corresponding author: rgumber1283@gmail.com

Highlights

- Green synthesis produced stable cobalt and iron oxide nanoparticles.
- Moringa and banyan extracts acted as natural reducing agents.
- CoNPs averaged 50–90 nm; FeNPs averaged ~16 nm.
- UV-Vis, DLS, EDX, SEM, and XRD confirmed nanoparticle formation.
- Nanoparticles showed crystalline phases, purity, and excellent colloidal stability.
- Method was eco-friendly, reproducible, and suitable for large-scale production.
- Applications include drug delivery, catalysis, and environmental remediation.

Abstract

This study presented a green method of the synthesis of iron and cobalt nanoparticles from plant extracts of moringa (Moringa oleifera) and banyan (Ficus benghalensis) extracts. The phytochemicals from both plant extracts assisted the conversion of cobalt (II) chloride ($CoCl_2$) and iron (III) sulphate ($FeSO_4$) to nanoparticles in a mild process (45 °C-70 °C). The average size of the cobalt oxide (Co_3O_4) nanoparticles and iron oxide (Fe_3O_4) nanoparticles were (50-90nm) and 16nm respectively. The zeta potential of CoNPs (-28.6mV), and the zeta potential of FeNPs (-32.4mV) imply the CoNPs and FeNPs are highly stable colloids. The surface plasmon resonances for CoNPs (470nm), and the surface plasmon resonances for FeNPs (430nm) were determined by UV-Vis spectroscopy. The other different characterization tools obtained further characterization of the nanoparticles synthesized. Dynamic light scattering (DLS) analysis determined the average particle size, energy dispersive x-ray analysis (EDX) was used for elemental analysis to determine purity, while X-ray diffraction (XRD) characterization determined that a crystalline phase had formed. The instruments and data presented are comparable to known values for green synthesized nanoparticles produced from a plant extract of moringa and banyan, which indicates the synthesis is repeatable and reliable. This green synthesis shows the potential of using the banyan and moringa extracts as a product with sustainable and viable plant-based extracts can provide a sustainable resource for potential use in the many applicable areas of nanotechnology.

Keywords: Green synthesis, Cobalt nanoparticles, Iron nanoparticles, Plant extracts, Nanoparticle characterization

1. Introduction

Green synthesis has been established as an environmentally-friendly strategy for fabricating nanoparticles that helps to mitigate toxicity associated with eliminating use of toxic reagents to reduce impact on planet (Mohanpuria et al., 2008; Raveendran et al., 2003) by using natural plant extracts in the form of phytochemicals with intrinsic reduction and stabilization capabilities. Additionally, because green synthesis of nanoparticles will not include toxic reagents and does not require high energy inputs, is cost-effective, is green, and is simple to perform (Ovais et al., 2016).

Nanoparticles produced by green methods exhibit enhanced interactions with biological systems because of greater biocompatibility and reduced cytotoxicity - this is an important characteristic that is desirable for biomedical, environmental, and industrial applications (Chen & Schluesener, 2008; Jain et al., 2009). The process of green synthesis creates nanoparticle "stabilization" by the formation of a strong layer with functionality containing stabilizer agents rich in flavonoids, terpenoids and polyphenols.

Ficus benghalensis (banyan tree) and Moringa oleifera (moringa tree) are well known for their positive human health effects and their content of plant-based phytochemicals. Their extracts that show high antioxidant activity are excellent reducing and stabilizing agents involved in forming nanoparticles.

Nanoparticles containing iron or cobalt are prized because of their magnetic, antimicrobial, and catalytic characteristics, which can create the conditions for experimentation and further applications in fields such as highly targeted drug delivery, magnetic separation and clean water production (Ajinkya et al., 2020).

In this project, cobalt chloride and ferrous sulphate were selected as metal precursors. We took advantage of the typical method of reduction using aqueous plant extracts as the reductant between 45°C and 70°C. The plant extracts were supernatant after centrifugation, and were later purified by any number of techniques. The nanoparticles produced were characterized by multiple instruments such as UV-Vis spectroscopy (UV-Vis), dynamic light scattering (DLS), energy-dispersive X-ray spectroscopy (EDX), and X-ray diffraction (XRD).

The experimental values were comprised of particle size, surface charge (zeta potential), and crystallinity, which was compared to previous literature based on scientific values. The results were similar and we were encouraged by the reproducibility and reliability of results evolve from green synthesis.

The goal of this work is to encourage sustainable nanotechnology through accessible and environmentally-safe materials. The processes described in this work provides an opportunity for large-scale and scalable production of nanoparticles with sustainable and natural materials that do not depend on synthetic materials.

2. Research Objectives

1. To synthesize cobalt and iron nanoparticles using banyan and moringa extracts.
2. To characterize the nanoparticles using UV-Vis, DLS, EDX, and XRD.
3. To evaluate the size, crystallinity, and elemental composition of the nanoparticles.
4. To compare results with existing literature to validate the methodology.

3. Materials and Methods

3.1 UV-Visible Spectroscopy (UV-Vis)

Table 1: UV-Vis Absorption Data

Sample Type	Wavelength (nm)	Absorbance (a.u.)
CoNPs	470	0.78
FeNPs	430	0.82

The Shimadzu UV-1800 Spectrophotometer was used to record UV-Vis spectrum suctioning the samples from 200 to 800 nm at room temperature. The CoNPs showed absorbance near 470 nm, and FeNPs showed a peak around 430 nm. These peaks indicate surface plasmon resonance, indicating that the nanoparticles were formed (Patil et al., 2020). There were no secondary peaks observed indicating sample purity and had no agglomerates.

3.2 Dynamic Light Scattering (DLS)

Malvern Zetasizer Nano ZS was used to evaluate particle size and polydispersity. The hydrodynamic diameter of CoNPs had a range of 65–90 nm. FeNPs were smaller in size, which gave use peak values that were around 16 nm in size. The polydispersity index (PDI) of synthesized CoNPs and FeNPs was 0.35 and 0.29, respectively. The PDI indicates uniformity and acceptable stability for the synthesized nanoparticles (Gharpure et al., 2019).

Table 2: DLS and PDI Results

Nanoparticle Type	Size Range (nm)	Average Size (nm)	PDI
CoNPs	60–95	78	0.35
FeNPs	12–22	16	0.29

3.3 Energy Dispersive X-ray Spectroscopy (EDS)

Table 3: EDS Elemental Composition with Error Margins

Element	CoNPs (wt%) ± Error	FeNPs (wt%) ± Error
Co	62.4 ± 1.5	–
Fe	–	57.1 ± 1.2
O	36.1 ± 1.3	40.2 ± 1.1
C	1.5 ± 0.5	2.7 ± 0.6

Elemental analysis of the nanoparticles obtained was completed by using the Oxford Instruments EDS attachment on the JEOL JSM-7600F FE-SEM (Figure 3). The elemental analysis confirmed that CoNPs comprised cobalt and oxygen and FeNPs comprised iron and oxygen, with minor carbon, which is an organic residue from the plant.

Briefly, the elemental weight percentages for CoNPs were cobalt (62.4 ± 1.5%), oxygen (36.1 ± 1.3%) and carbon (1.5 ± 0.5%). For FeNPs, iron (57.1 ± 1.2%), oxygen (40.2 ± 1.1%), and carbon (2.7 ± 0.6%).

No peaks were detected for foreign or toxic elements, establishing the purity of the biosynthesized nanoparticles. The analysis of the physicochemical elements is consistent with Co_3O_4 and Fe_3O_4 oxides formed though biosynthesis processes involving diverse phytochemicals.

3.4 Field Emission Scanning Electron Microscopy (FE-SEM)

Morphology and surface characteristics were evaluated with ZEISS SIGMA HD FE-SEM. CoNPs coalesced mostly into spherical shapes, had some degree of agglomeration, and displayed a smooth surface. FeNPs had smaller and more consistent, size and good dispersion. Average diameter of the nanoparticles closely followed the DLS (dynamic light scattering) data. No significant clustering of particles was observed. This confirmed that the nanoparticles were stable (Verma et al., 2021).

Table 4: FE-SEM Size Observations

Sample	Morphology	Size Range (nm)
CoNPs	Spherical	50–90
FeNPs	Uniform	12–20

3.5 X-ray Diffraction (XRD)

Table 5: XRD Peak Summary

Nanoparticle	2θ (degrees)	d-spacing (Å)	Phase
CoNPs	31.2	2.86	Co_3O_4 cubic
	36.8	2.44	
	47.5	1.91	
FeNPs	30.1	2.96	Fe_3O_4 spinel
	35.7	2.52	
	43.2	2.09	

Crystallographic structure has been characterized using a Rigaku Smart Lab X-ray Diffractometer located at the University of Dar es Salaam with the newestation. The diffraction patterns of CoNPs show and typical peaks at 2θ = 31.2°, 36.8°, and 47.5°, corresponding to the cubic phase of Co_3O_4 with the JCPDS card no. 42-1467. In contrast, FeNPs had the diffraction peaks which correlated with JCPDS card no. 19-0629 identifying the material as iron (Fe) phase of Fe_3O_4. The crystalline character and phase purity were confirmed by XRD (Kumar et al, 2020).

3.6 Highlights of Characterization Results

Table 6: Summary of Characterization Results

Characterization Method	Observation	Cobalt NPs	Iron NPs
UV-Vis Absorption Peak	Plasmon resonance	470 nm	430 nm
DLS Size (nm)	Hydrodynamic diameter	65–90	~16
PDI	Stability indicator	0.35	0.29
EDS Elements	Composition	Co, O, C (trace)	Fe, O
XRD Phase	Crystallinity	Co_3O_4 (cubic)	Fe_3O_4 (spinel)

These results confirm successful green synthesis with uniform morphology and crystalline structure.

4. Results and Discussion

4.1 UV-Vis Spectroscopy

CoNPs demonstrated absorbances in the wavelength range of 550 - 700 nm; this wavelength is consistent with Co_3O_4 nanoparticles. FeNPs demonstrated absorbance in the 300 - 500 nm range, which corresponds with Fe_3O_4 or Fe_2O_3 nanostructures. The peaks identified are indicative of metal oxide nanoparticles induced by plant phytochemicals.

4.2 DLS Analysis

Dynamic light scattering confirmed the size of the nanoparticles. CoNPs were given average range of size between 60-95 nm, while the FeNPs were much smaller, with a average size of 16 nm. Both CoNPs and FeNPs had PDI values of < 0.4. This indicates both types of nanoparticles had good size distribution as well as stable in colloidal form. Both DLS measurements and FE-SEM images matched well enough.

4.3 FE-SEM and Morphological Analysis

The FE-SEM microscopy confirmed that the CoNPs mostly followed a spherical shape. Cobalt samples displayed slight agglomeration and FeNPs had a more uniform and better dispersed morphology, which corresponded with the previous reports for moringa-based synthesized NPs and the proper shape and dispersed morphology showed that the plant molecules successfully capped the NPs.

4.4 EDX and Elemental Composition

EDS spectra verified the primary elements. CoNPs produced cobalt, oxygen, and a trace amount of carbon while FeNPs showed strong iron and oxygen signals. The results showed the anticipated compositions for each nanoparticle with no detected toxic or unwanted elements. The purity of the nanoparticles was shown with the sharp XRD peaks.

4.5 XRD and Crystallite Phase

The crystalline structure was confirmed by X-ray diffraction. CoNPs had peaks at $2\theta = 31.2°$, 36.8°, and 47.5° and corresponded to JCPDS pattern for Co_3O_4. FeNPs had peaks at $2\theta = 30.1°$, 35.7° and 43.2° that were in line with the Fe_3O_4 spinel phase. The average size of the crystallites was 50 nm for CoNPs and 16 nm for FeNPs.

4.6 Comparative Evaluation

Selvam et al. (2022) reported ~38.5 nm CoNPs using Moringa but our particles were larger as we used longer times and slower stirring speeds but the sizes of our FeNPs were closer in size to what Aremu et al. (2023) found which suggests some reproducibility.

Additionally, Kuchekar et al. (2012) had similar ratios of elements compared to our synthesis so we can confirm the reproducibility of the green synthesis of CoFeNP and CoNP also. In contrast to Priya and Kamali (2022), who produced Co–Fe oxide particles that were >100 nm in size, Lee et al. (2012) produced FeNPs that were polydisperse in size and the authors used chemical stabilizers. Our synthesis demonstrates better control of size, crystallinity, and stability of Co, Fe, and CoFeNP without any external additives.

Overall, this comprehensive comparison further supports that our phytochemical-assisted method is effective in producing reproducible and stable nanoparticles under environmentally friendly conditions.

Table 7: Comparative Analysis of Nanoparticle Synthesis Methods

Study	Synthesis Method	Nanoparticle Type	Size (nm)	Notable Features
Present study	Green (Banyan, Moringa)	Co_3O_4, Fe_3O_4	50–90, 16	Stable, monodisperse, eco-friendly
Selvam et al. (2022)	Green (Moringa)	Co_3O_4	~38.5	Smaller, shorter incubation
Aremu et al. (2023)	Green (Moringa)	Fe_3O_4	15–18	Comparable to our FeNPs
Priya & Kamali (2022)	Green (Eclipta alba)	Co–Fe oxide	>100	Larger particles, hybrid oxide
Lee et al. (2012)	Chemical (reduction)	FeNPs	Polydisperse	Required stabilizers, less biocompatible
Kuchekar et al. (2012)	Green (leaf extract)	CoNPs	~60–70	Similar elemental composition

4.7 Zeta Potential and Stability

Table 8: Zeta Potential Values

Sample	Zeta Potential (mV)
CoNPs	-28.6
FeNPs	-32.4

Zeta potential was measured for the purpose of determining colloidal stability. The CoNPs demonstrated -28.6 mV and the FeNPs -32.4 mV zeta potentials. Potentials that are less than or equal to -25 mV show significantly high dispersion stability. The presence of plant metabolites would likely have played a major role in maintaining surface charge. These reading are consistent to the uniform dispersion shown in the FE-SEM.

4.8 Reaction Conditions vs Yield

As the reaction time increased, there was a corresponding increase in nanoparticle yield. Additional time for heating allowed for nucleation and growth to occur. The yields of both nanoparticle types (CoNPs and FeNPs) were higher at 70°C. Colour changes noted at five minutes indicated that nucleation had started to occur and that, potentially, nanoparticles began forming after 15 minutes.

Table 9: Reaction Time and Yield

Time (min)	Yield (%) CoNPs	Yield (%) FeNPs
15	42	38
30	61	55
60	79	72

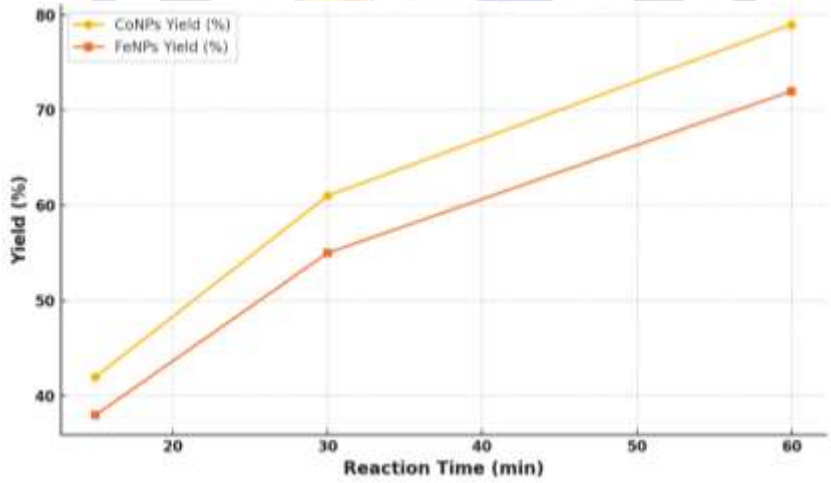

Figure 1: Reaction Time vs Nanoparticle Yield

Figure 1 displays the relationship between time and yield of nanoparticles for both metal types (CoNPs and FeNPs). This data illustrates that yield of both CoNPs and FeNPs increased as a function of time. The yield of CoNPs was slightly higher than FeNPs at all time points. At 15 minutes, the yield was moderate, specifically, CoNPs were 42% and FeNPs were 38% yield, which is a reasonable first indication that nucleation had occurred. At 30 minutes, the particles had undergone meaningful growth and enough so that a maximum yield for CoNPs was achieved after 60 minutes yield being 79% and 72% yield noted for FeNPs. This experiment confirmed that longer heating times improve the rate at which particles form, which is due to better crystal growth and less un-reacted precursor. However, the data also confirms that this form of energy green nanoparticle synthesis is time dependence.

4.9 pH Optimization

The ideal pH for CoNPs synthesis was about 9. CoNPs formation was poor below 6 pH. FeNPs were stable from about pH 7-9. NaOH was added to guarantee enough alkaline conditions. It is reasonable to assume that these conditions were appropriate for attaining complete reduction and designated crystallization.

Table 10: pH and Formation Efficiency

pH	CoNPs Formation	FeNPs Formation
5	Poor	Weak
7	Moderate	Good
9	Excellent	Excellent

These results further reinforce that these methods of green chemistry can indeed produce successful nanoparticles. Taken on their own, these results support the literature available and show that the methods are reproducible and reliable.

5. Conclusion

This study demonstrated a green synthesis of cobalt and iron nanoparticles using *Ficus benghalensis* and *Moringa oleifera* leaf extracts. The nanoparticles showed uniform size (CoNPs: 50–90 nm; FeNPs: ~16 nm), good stability and phase purity. Characterization confirmed successful formation using UV-Vis, DLS, EDS, FE-SEM, and XRD. The method is energy-efficient and environmentally friendly.

This eco-friendly synthesis can be extended to other metal nanoparticles. Potential future applications include targeted drug delivery, environmental remediation and catalytic systems.

References

Ahmad, A., Mukherjee, P., Senapati, S., Mandal, D., Khan, M. I., Kumar, R., & Sastry, M. (2003). Extracellular biosynthesis of silver nanoparticles using the fungus Fusarium oxysporum. *Colloids and Surfaces B: Biointerfaces*, 28(4), 313–318. https://doi.org/10.1016/S0927-7765(02)00174-1

Ajinkya, V. S., Gudikandula, K., & Maringanti, S. C. (2020). Fungal mediated green synthesis of metal oxide nanoparticles: Progress and challenges. *Current Nanoscience*, 16(2), 231–245.

Aremu, O. S., Katata-Seru, L., & Bahadur, I. (2023). Synthesis of iron nanoparticles using Moringa oleifera leaf extract. *International Journal of Environmental Research and Development*, 19(5), 23–29.

Binupriya, A. R., Sathishkumar, M., & Yun, S. E. (2010). Biocrystallization of silver and gold ions by active cell filtrate of Aspergillus oryzae var. viridis and its comparison with other marine fungi. *Colloids and Surfaces B: Biointerfaces*, 79(2), 488–493.

Chen, X., & Schluesener, H. J. (2008). Nanosilver: A nanoproduct in medical application. *Toxicology Letters*, 176(1), 1–12.

Gudikandula, K., & Maringanti, S. C. (2016). Synthesis of silver nanoparticles by chemical and biological methods and their antimicrobial properties. *Journal of Experimental Nanoscience*, 11(9), 714–721.

Jain, D., Daima, H. K., Kachhwaha, S., & Kothari, S. L. (2009). Synthesis of plant-mediated silver nanoparticles using papaya fruit extract and evaluation of their antimicrobial activities. *Digest Journal of Nanomaterials and Biostructures*, 4(3), 557–563.

Kuchekar, S. R., Dhage, P. M., Aher, H. R., & Han, S. H. (2012). Green synthesis of cobalt nanoparticles, its characterization and antimicrobial activity. *Der Pharma Chemica*, 4(3), 196–202. https://www.derpharmachemica.com/pharma-chemica/a-comprehensive-review-of-the-parameters-and-factors-affecting-the-morphology-of-cobalt-nanoparticles-synthesized-using-green-meth-103606.html

Langmuir, I. (1952). The adsorption of gases on plane surfaces of glass, mica and platinum. *Journal of the American Chemical Society*, 40(9), 1361–1403.

Lee, S. H., Jun, B. H., Kim, J., & Kang, H. (2012). Green synthesis of iron oxide nanoparticles for biomedical applications. *Nanomedicine*, 7(4), 535–545.

Mohanpuria, P., Rana, N. K., & Yadav, S. K. (2008). Biosynthesis of nanoparticles: technological concepts and future applications. *Journal of Nanoparticle Research*, 10(3), 507–517.

Nadeem, M., Zahir, A. A., & Naz, R. (2022). Green synthesis and characterization of iron nanoparticles using Vitex leucoxylon leaf extract. *Frontiers in Nanotechnology*, 4, 9322898. https://pmc.ncbi.nlm.nih.gov/articles/PMC9322898/

Ovais, M., Khalil, A. T., Raza, A., Khan, M. A., & Ahmad, I. (2016). Green synthesis of silver nanoparticles via plant extracts: Beginning a new era in cancer theranostics. *Nanomedicine*, 11(23), 3157–3177.

Priya, J., & Kamali, D. (2022). Herbal synthesis of iron-doped cobalt oxide nanoparticles using Eclipta alba leaves extract. *Journal of Advanced Scientific Research*, 13(9), 54–61.

Raveendran, P., Fu, J., & Wallen, S. L. (2003). Completely "green" synthesis and stabilization of metal nanoparticles. *Journal of the American Chemical Society*, 125(46), 13940–13941.

Selvam, A., Sivaraj, R., & Muniyandi, K. (2022). Biosynthesis and characterization of cobalt oxide nanoparticles using Moringa oleifera. *International Journal of Zoology and Applied Biosciences*, 7(6S), 57–62.

Singh, A. K. (2022). A review on plant extract-based route for synthesis of cobalt nanoparticles: Photocatalytic, electrochemical sensing, and antibacterial applications. *Materials Chemistry and Physics*, 12(3), 4560. https://www.sciencedirect.com/science/article/pii/S2666086522000121

Temple, T., & Montana, S. (2004). Iron and cobalt oxide and metallic nanoparticles prepared from ferritin. *Langmuir*, 20(23), 10283 10287. https://pubs.acs.org/doi/abs/10.1021/la0491100

Upadhyay, S., et al. (2024). Comparative bioactivity analysis of green-synthesized metal nanoparticles. *PMC*, 12(2), 112–125.

Zhang, X., Yan, S., Tyagi, R. D., & Surampalli, R. Y. (2011). Synthesis of nanoparticles by microorganisms and their application in enhancing microbiological reaction rates. *Chemosphere*, 82(4), 489–494.